Mixed-mode oscillations and cluster patterns in an electrochemical relaxation oscillator under galvanostatic control

Nilüfer Baba and Katharina Krischer[a]

Physik Department E19, Technische Universität München, James Franck Strasse 1,
85748 Garching bei München, Germany

We studied the dynamics of a prototypical electrochemical model, the electro-oxidation of hydrogen in the presence of poisons, under galvanostatic conditions. The lumped system exhibits relaxation oscillations, which develop mixed-mode oscillations (MMOs) for low preset currents. A fast-slow analysis of the homogeneous dynamics reveals that the MMOs arise from a fast oscillating subsystem and a one-dimensional slow manifold. In the spatially extended system, the galvanostatic constraint imposes a synchronizing global coupling that drives the system into cluster patterns. The properties of the cluster patterns (CPs) result from an intricate interplay of the nature of the local oscillators, the global constraint, and a nonlocal coupling through the electrolyte. In particular, we find that the global constraint suppresses small-amplitude oscillations of MMOs and prevents domains oscillating out of phase from occupying equal regions in phase space. The nonlocal coupling causes each individual clustered region to oscillate on a different limit cycle. Typically multistability of CPs is found. Coexisting patterns possess different oscillation periods and a different total fraction in space that occupies the in-phase or out-of-phase state, respectively. © *2008 American Institute of Physics*. [DOI: 10.1063/1.2779856]

Globally coupled oscillators have been studied extensively and have helped us to understand important concepts of synchronization. In spatially extended systems, global coupling acts always together with (non)local coupling. As a consequence, spatially coherent structures without an intrinsic wavelength occur. Globally coupled oscillatory media, e.g., form cluster patterns (CPs) that are characterized by synchronized domains that exhibit a constant phase shift among each other. Many properties of these patterns are still unknown. Among the open questions are, what determines the relative total size of different domains, or what is the relation of the period of a local oscillation in a CP and the period of the homogeneous oscillation? Global coupling is present in most electrochemical systems, cluster states being a prominent pattern observed experimentally. We study theoretically pattern formation in a prototypical electrochemical model with global coupling. The underlying homogeneous system is four-dimensional and exhibits besides simple periodic oscillations also mixed-mode oscillations. CPs arising in the spatially extended model are analyzed with the focus on extracting rules that govern the different properties of the patterns.

I. INTRODUCTION

Electrochemical systems have proven to exhibit a wide variety of dynamical behaviors[1,2] and have served for a long time as prototypical systems in experimental studies of complex dynamics, such as mixed-mode oscillations (MMOs),[3–9] synchronization phenomena of globally coupled oscillators,[10,11] or the impact of nonlocal coupling on pattern formation.[12–17] In this context, an advantageous property of electrochemical systems is that both global and (non)local coupling can be easily varied experimentally in wide ranges.

Global coupling comes about by the external control of an electrochemical system. When the total current flowing through the electrochemical cell is kept constant, an operation mode that is called galvanostatic control, a positive (synchronizing) global coupling is introduced.[18] This can be seen easily: If the reaction current density changes locally at some position on the electrode, e.g., due to a local fluctuation, so obviously does the total reaction current density. Consequently, the galvanostatic control device shifts the potential of the electrode such that the resulting capacitive current is equal to the difference between the preset current and the total reaction current. Thus, a change of the local properties of the electrode instantaneously affects the dynamics at all positions. Under so-called potentiostatic conditions, a constant voltage between the working electrode (WE) and the reference electrode (RE) is applied. If there is an external resistor in the outer circuitry, it introduces in the same way as the galvanostatic control a positive global coupling. The strength of the coupling can now be tuned through the magnitude of the external resistance. If, on the other hand, the RE is brought close to the WE, or a negative impedance device is connected in series to the WE, a desynchronizing global coupling is introduced.[19,20] In this case, the coupling strength can be varied by changing the distance between the RE and the WE or the magnitude of the impedance, respectively.

Nonlocal coupling is mediated via the electrostatic potential in the electrolyte.[21] The potential drop across the elec-

[a]Electronic mail: krischer@ph.tum.de.

trochemical interface is an essential variable for the dynamics of most electrochemical systems. If it changes locally, this change prompts a redistribution of the electrostatic potential in the entire electrolyte and, therefore, of the electric field at the electrode. This, in turn, affects the migration current density entering the interface. In this way, different positions of the interface are coupled with each other. The strength of the coupling depends on the distance of a location to the reference location, but it is not restricted to the immediate neighborhood of the reference position. Thus migration coupling is a nonlocal coupling.

An electrochemical model system, with which much insight into the impact of nonlocal and global coupling on pattern formation could be obtained, is the hydrogen oxidation in the presence of Cu^{2+} and Cl^- ions on a Pt electrode. Its local dynamics is well understood.[22] It involves the adsorption of the two ionic species, which both inhibit oxidation of hydrogen when adsorbed. Owing to their opposite potential dependence of the adsorption, one of them, Cl^-, takes part in the positive feedback loop, whereas Cu^{2+} is an essential species of the inhibitory, negative feedback loop. Based on these electrochemical steps, a mathematical model was proposed[22] that proved to yield nearly quantitative results even when complex spatio-temporal patterns were considered.[14,15]

While all former theoretical studies with this model were done for potentiostatic control and desynchronizing global coupling, in this paper we focus on galvanostatic conditions. After the introduction of the model equations in the following section, we demonstrate in Sec. III that the model predicts MMOs of the homogeneous system; applying a fast-slow analysis reveals that the MMOs are of the bursting-type, i.e., that the MMOs arise due to a fast oscillatory subsystem that is coupled to a slowly evolving variable. This allows us to investigate the impact of a positive global coupling in an active medium with bursting oscillations, which is done in Sec. IV. The dominant patterns we find are CPs in which the mixed-mode character of the local oscillations is strongly suppressed. Furthermore, the CPs have some features that to our knowledge discriminate them from other CPs described in the literature. It is proposed that the suppression of the MMOs as well as several of the other unusual cluster features are the results of the imposed galvanostatic constraint. Thus, several properties of the CPs described here should be characteristic for systems with a global constraint, as opposed to a global feedback that was present in the other studies of CPs in spatially extended media. Further characteristics can be traced back to the nonlocal coupling. Conclusions and an outlook are given in Sec. V.

II. MODEL

We employed the model introduced by Plenge *et al.*[15,22] to describe the dynamics of the hydrogen oxidation reaction in the presence of Cu^{2+} and Cl^- ions on a Pt electrode. In dimensionless form, the model reads

$$\dot{\phi}_{DL} = -i_r - \frac{\sigma}{\beta}\frac{\partial \phi}{\partial z}\bigg|_{z=0}, \tag{1}$$

$$\dot{\theta}_{Cl} = \tau_{Cl}^{-1}[(1+\chi\theta_{Cu})(1-\theta_{Cu}-\theta_{Cl})e^{\phi_{DL}} - p_{Cl}\theta_{Cl}e^{-\phi_{DL}}], \tag{2}$$

$$\dot{\theta}_{Cu} = \tau_{Cu}^{-1}(v_{Cu}^a - v_{Cu}^d), \tag{3}$$

$$\dot{c}_{Cu} = 1 - c_{Cu} - \nu\tau_{Cu}^{-1}(v_{Cu}^a - v_{Cu}^d), \tag{4}$$

with

$$v_{Cu}^a - v_{Cu}^d = c_{Cu}(1-\theta_{Cu}-\theta_{Cl})e^{-a_{Cu}\phi_{DL}} - p_{Cu}\theta_{Cu}e^{a_{Cu}\phi_{DL}},$$

$$i_r = c_1(1-\theta_{Cu}-\theta_{Cl})[1-2(1+e^{c_2\phi_{DL}})^{-1}].$$

Here, ϕ_{DL} denotes the potential drop across the double layer, or, in short, the double-layer potential. Equation (1) results from a local charge balance and states that ϕ_{DL} changes whenever the reaction current density i_r does not match the local migration current density at the WE i_m. z is the direction normal to the WE pointing into the electrolyte and $z=0$ is a location at the WE. i_m depends on two parameters—the conductivity σ and the aspect ratio of the electrochemical cell β—and is expressed in terms of the electrostatic potential in the electrolyte, ϕ. Since the electrolyte is an electroneutral medium, ϕ can be obtained to a very good approximation from Laplace's equation ($\Delta\phi=0$). In the calculations, we considered a quasi-one-dimensional ring WE and solved Laplace's equation on a cylindrical surface that was bounded from the top and the bottom by the WE and the counter electrode (CE), respectively.[18] In the following, the angular coordinate is denoted by x, with $x\in[0,2\pi]$. Potential variations at the CE (located at $z=1$) can be neglected and it is convenient to set $\phi|_{z=1}=0$.

The relation between ϕ_{DL} and ϕ results from the considered control mode. Under galvanostatic conditions, the following constraint is imposed:

$$\frac{\sigma}{\beta}\int_x \frac{\partial\phi}{\partial z}\bigg|_{z=0} dx = i_0,$$

where i_0 is the preset current density and the integration is over the entire electrode.

θ_{Cu} and θ_{Cl} denote the surface coverages of copper and chloride on the Pt electrode, and the terms on the right-hand side of Eqs. (2) and (3) describe the respective adsorption and desorption kinetics (for details, see Ref. 22). Treating the concentration of copper ions in front of the electrode, c_{Cu}, as a variable ensures nearly quantitative agreement between experimental and simulated homogeneous oscillations. Its temporal evolution is determined by diffusion of Cu^{2+} ions to and from the bulk electrolyte, on the one hand, and adsorption and desorption fluxes at the electrode, on the other hand. Compared to migration coupling, spatial coupling through diffusion of any of the three chemical species is negligible and was not considered in the simulations. For further explanations of the parameters and physical meanings of the terms in Eqs. (1)–(4), see Ref. 22. In the present paper, the parameters were fixed to the following values: $\tau_{Cu}=21.032\,15$, $\tau_{Cl}=83\,760.090$, $p_{Cl}=497.864\,24$, $p_{Cu}=3.139\,13\times10^{-15}$, $\chi=50$, $c_1=4.897\,46$, $c_2=39.553\,36$, $\nu=17\,401.491\,97$, a_{Cu}
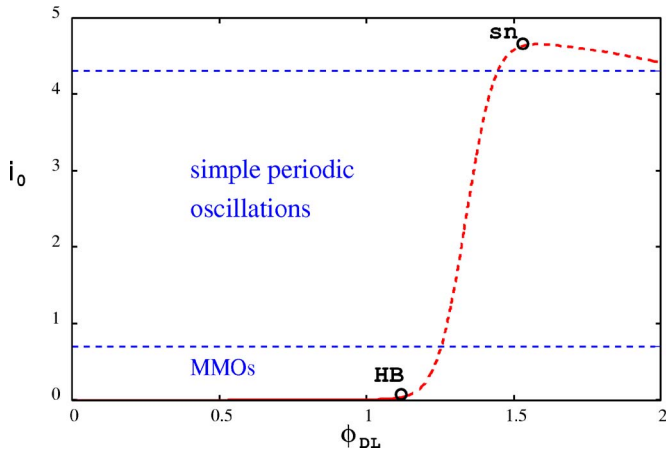
FIG. 1. (Color online) Current-voltage curves of the stationary homogeneous steady states under galvanostatic conditions calculated with model Eqs. (1)–(4) and existence range of MMOs and simple periodic oscillations in the homogeneous model. Dashed line: unstable steady state (sn: saddle node bifurcation; HB: Hopf bifurcation). Parameters: see Sec. II.

$= 12.666\,67$, and $\beta = 1.8$. These values are gained from typical parameter values used in the experiments.

For the chosen cell geometry, the eigenfunctions of the Laplace operator along the azimuthal direction are Fourier functions.[12] Expanding all variables in a Fourier series, evolution equations for the Fourier coefficients are obtained. The resulting set of ordinary differential equations was integrated using lsode.[23] Either 64 (Figs. 4 and 5) or 128 (Figs. 6–8) Fourier modes were used; the number of allocation points in real space was four times larger than the number of Fourier modes.

III. MIXED-MODE OSCILLATIONS IN THE HOMOGENEOUS SYSTEM

First, we consider the dynamics of the spatially homogeneous system under galvanostatic control. In this case, Eq. (1) becomes

$$\dot{\phi}_{DL} = -i_r + i_0. \qquad (5)$$

The corresponding set of ordinary differential equations (ODEs) [Eqs. (2)–(5)] exhibits oscillations in nearly the entire physically meaningful range of the preset current density i_0, our main bifurcation parameter. At low values of i_0, the oscillations are of the mixed-mode type, while at higher current densities, simple periodic oscillations prevail. A current-voltage characteristic of the stationary steady states is shown in Fig. 1 together with the ranges of current densities, in which simple periodic and MMOs, respectively, exist. At low currents, the stationary state becomes unstable via Hopf bifurcation (HB); the resulting unstable fixed point is destroyed at high current densities in a saddle node (sn) bifurcation.

For a deeper understanding of the spatio-temporal patterns discussed below, it is necessary to understand the mechanism generating the MMOs in the homogeneous model. This is a difficult task in the full four-variable model. All qualitative features of the MMOs, however, persisted when c_{Cu} was set to 1. The resulting three-dimensional
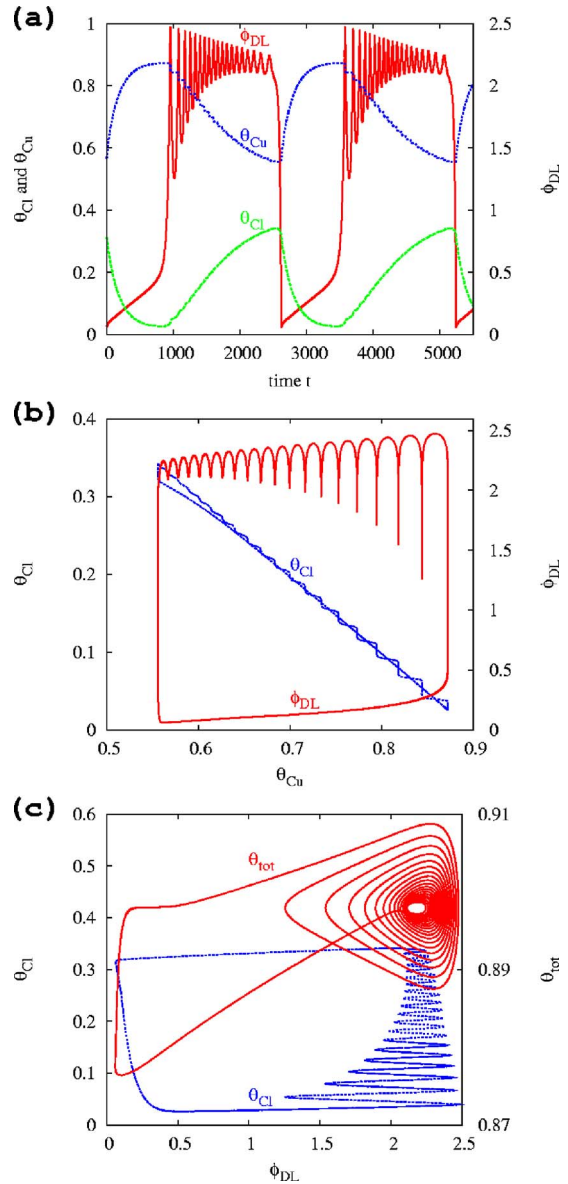

FIG. 2. (Color online) Appearance of MMO in the three-dimensional model of $H_2|Cl^-, Cu^{2+}, H_2SO_4|Pt$ under galvanostatic control for $i_0 = 0.5$ and $c_{Cu} = 1.0$. Comparison of the time series of ϕ_{DL}, θ_{Cl}, and θ_{Cu} (a) and different projections of the trajectory onto different planes in phase space [(b) and (c)]. (c) reveals that ϕ_{DL} and θ_{tot} span the fast subsystem.

model exhibits similar MMOs in almost the same parameter range as the full model. Time series of MMOs calculated with the three-dimensional model are shown in Fig. 2(a), and projections of the attractor onto different two-dimensional phase-space planes are depicted in Figs. 2(b) and 2(c).

Looking at the time series, it is striking that only the one of ϕ_{DL} exhibits the typical features of MMOs, namely small-amplitude oscillations (SAOs) that are interrupted by large-amplitude excursions; θ_{Cu} decreases and θ_{Cl} increases monotonically when ϕ_{DL} exhibits SAOs. As a result, also none of the projections of the attractor onto any plane spanned by the "natural coordinates" [Figs. 2(b) and 2(c), blue line] exhibits limit-cycle-type small-amplitude structures. These only appear after a suitable variable transformation, namely when replacing θ_{Cl} by the total coverage $\theta_{tot} = \theta_{Cl} + \theta_{Cu}$. A projec-
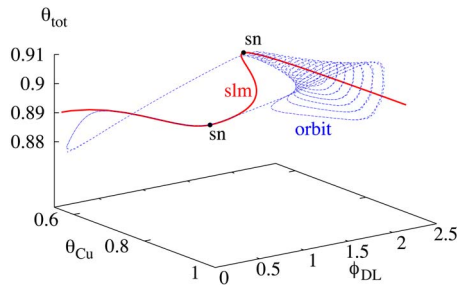
FIG. 3. (Color online) Mixed-mode orbit of the three-dimensional model on a one-dimensional S-shaped slow manifold (curve labeled slm). sn denotes saddle node bifurcation of the slow manifold. Parameters: $i_0 = 0.5$, $c_{Cu} = 1.0$.

tion of the attractor onto the phase plane spanned by $(\theta_{tot}, \phi_{DL})$ [Fig. 2(c), red curve], reveals that the SAOs are connected with a damped oscillatory motion in the $(\theta_{tot}, \phi_{DL})$ plane; however, instead of settling to a stationary value, the limit cycle trajectory undergoes a large excursion in phase space, or a large-amplitude oscillation. These features suggest that the MMOs are associated with a saddle focus that has a two-dimensional oscillatory inset. But the three-dimensional model does not possess a fixed point in this region of phase space. Additional model reductions help to further elucidate the phase space structure.

The time series of ϕ_{DL} [Fig. 2(a)] undergoes fast transitions between a slowly varying low-potential and an oscillatory high-potential branch, while θ_{Cu} and θ_{Cl} decrease or increase slowly, depending on which branch ϕ_{DL} is. This suggests that ϕ_{DL} is a fast variable and the dynamical system has multiple time scales. Unfortunately, there is no simple transformation that would allow us to extract a small parameter proportional to the ratio of time scales and to subsequently do a rigorous analysis of the slow and fast subsystems. But obviously, the dynamics of θ_{Cu} is much slower than that of ϕ_{DL} and θ_{tot}; thus, the latter two variables form a fast subsystem.

The one-dimensional slow manifold can be calculated by treating θ_{Cu} as a bifurcation parameter and solving for the steady states of the remaining two-dimensional system. One obtains an S-shaped curve with the middle unstable branch bordered by two saddle node bifurcations (Fig. 3, red, thick line). The stable steady states on the high ϕ_{DL} branch are stable foci. A mixed-mode limit cycle exhibits damped SAOs in ϕ_{DL} and θ_{tot} around this upper branch while θ_{Cu} decreases slowly. Once the sn is reached, the trajectory jumps to the low ϕ_{DL} branch of the slow manifold on which it remains while now θ_{Cu} slowly increases. In this way, the trajectory reaches the lower sn, which, in turn, triggers a jump into the basin of influence of the upper focus and the cycle starts anew (Fig. 3, blue, thin line). The MMOs are thus the result of the interaction of a fast oscillatory subsystem with a one-dimensional slow S-shaped manifold. These types of MMOs are often referred to as bursting oscillations; see e.g., Refs. 24 and 25.

IV. CLUSTER PATTERNS IN THE SPATIALLY EXTENDED SYSTEM

In the spatially extended system [Eqs. (1)–(4)], pattern formation is observed in large parameter regions. Under gal-
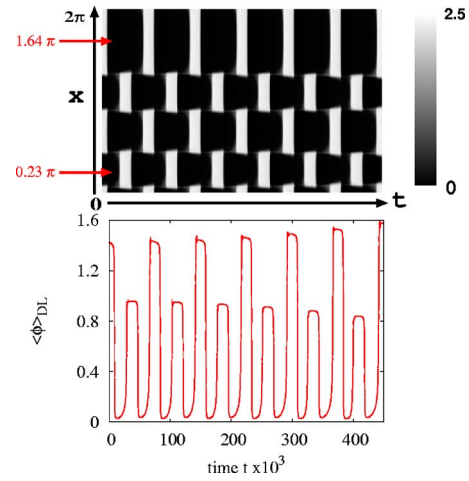

FIG. 4. (Color online) Transient CPs in the MMO regime. Parameters: $i_0 = 0.5$, $\beta = 1.8$, and $\sigma = 0.03$; initial condition: state on the uniform limit cycle with low amplitude noise superimposed.

vanostatic control, dominantly CPs are found. CPs are characterized by the presence of a small number of oscillating, synchronized domains that exhibit among each other a certain phase shift and possess possibly different oscillation amplitudes. A simple classification of CPs distinguishes between phase clusters and amplitude clusters. In the former, the oscillation amplitude is equal for all cluster regimes, while different oscillating regions of the latter have also different amplitudes. CPs are a signature of global coupling. In our case, the global coupling is imposed by the galvanostatic control mode.[18]

A typical example of CPs emerging in the mixed-mode regime of the homogeneous model is displayed in Fig. 4. The pattern evolved from a noisy homogeneous initial condition. It consists of four domains, however they are apparently pairwise synchronized so that to a first approximation we are dealing with a two-state CP. As is typical for CPs, there is no characteristic wavelength. However, in spatially extended systems both cluster states were reported to tend to occupy the same total domain size, a phenomenon that has been termed phase balance.[26–28] As a consequence, spatially averaged quantities exhibit simple periodic oscillations with twice the frequency of the local oscillators. As is obvious from a visual inspection of the space-time data and the time series of the average double-layer potential in Fig. 4, phase balance is not reached in our CPs. Besides, from the time series it becomes apparent that the system has not yet reached an asymptotic state. Rather, the state already occupying the larger area slowly grows at the expense of the other one. We confirmed that this trend continues until the electrode has reached a uniform state. Thus, at these parameter values, as well as at all other ones in which the homogeneous system exhibited MMOs, the CPs are not stable solutions. Note, however, that the CPs emerged after applying small random fluctuations to a uniform state, which indicates that they can be excited easily. Stable CPs existed at larger values of i_0, at which the homogeneous model has simple periodic oscillations.
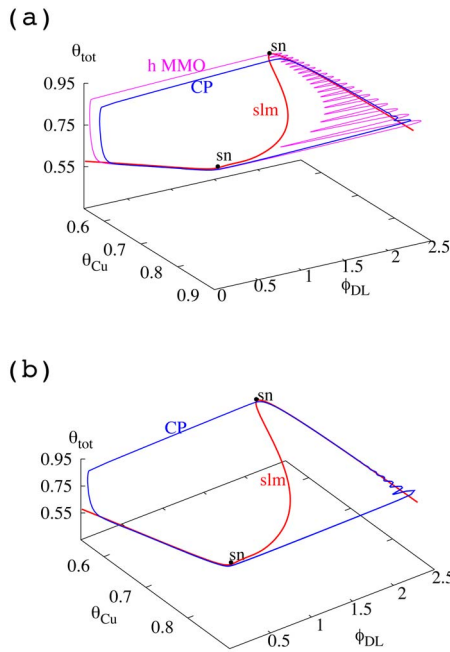
FIG. 5. (Color online) Trajectories in phase space of local oscillations (curves labeled CP) of the CP shown in Fig. 4 (a) at the position x =0.23 π and (b) at the position x=1.64 π. The respective curves labeled slm are the slow manifold of the homogeneous system (for their calculation, see Sec. III). The orbit (curve labeled h MMO) in (a) shows for comparison the stable MMO limit cycle of the homogeneous system.

Before discussing these stable cluster solutions in more detail, it is instructive to look at two local oscillations with antiphase behavior in phase space (Fig. 5, blue lines). The trajectories follow closely the stable branches of the slow manifold, as one might have expected. However, two features of the phase portraits are surprising: First, the SAOs on the upper branch of the local cluster oscillators are much less pronounced than for the homogeneous oscillation at the same parameter values. For comparison, the latter one is shown in red in Fig. 5(a). This was typical for all CPs in the MMO region. We will come back to this point below. Second, the two oscillators do not trace out equal paths in phase space. Rather, the upper one, which belongs to a point within the less extended domain, exhibits the transition from the upper to the lower ϕ_{DL} branch before the trajectory has reached the sn bifurcation of the slow manifold. In addition, here the SAOs are even less pronounced than in the lower phase portrait, corresponding to a point of the larger domain in Fig. 4. We thus conclude that the oscillators of the two states are not identical.

Examples for stable CPs at a higher value of i_0, at which the uniform system exhibits simple periodic oscillations that do not trace out the slow manifold anymore, are displayed in Fig. 6. They exhibit several remarkable features. First, the two patterns were obtained for different initial conditions but otherwise identical parameters. They obviously differ in the total fraction of the electrode occupied by each cluster state, and also possess different periods of local and global oscillations. Thus, there is a multiplicity of patterns.

Second, both patterns are far from being phase-balanced. In fact, in none of our calculations did we find a phase-
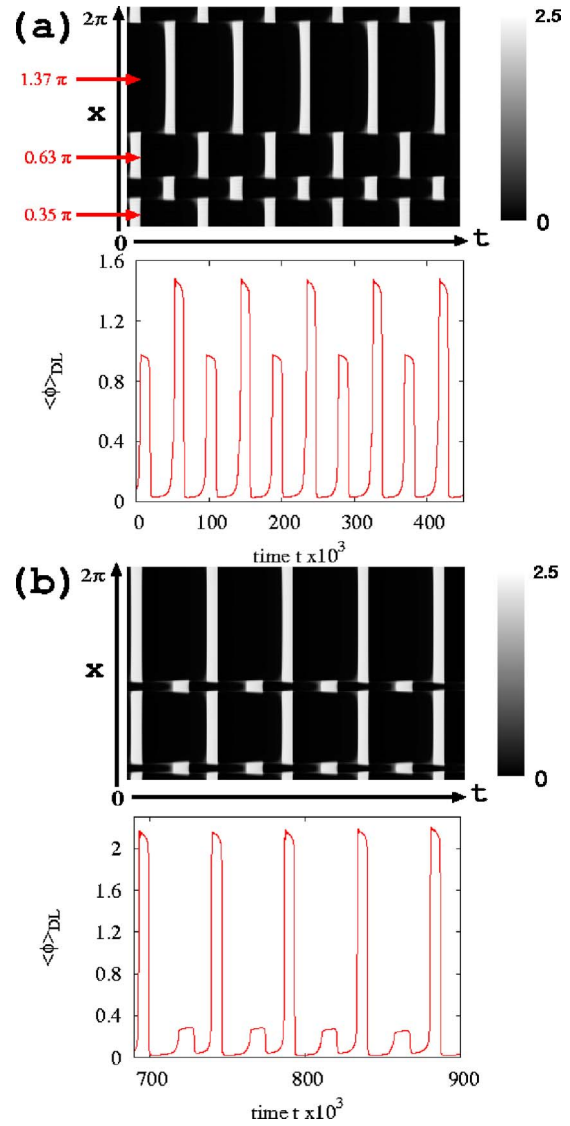

FIG. 6. (Color online) Multiplicity of stable CPs beyond the MMO regime of the homogeneous system. Upper plates: Pseudocolor representation of the spatio-temporal evolution of the double-layer potential; lower plates: time series of the average double-layer potential. Initial conditions: (a) Uniform state of the homogeneous system with low amplitude noise superimposed. The arrows indicate the positions at which local trajectories and time series in Figs. 7 and 8 are taken; (b) half of the domain was set in one of the two cluster states of the upper plate, the other half in the other cluster state. Parameters for both patterns: i_0=1.0, σ=0.02, and β=1.8.

balanced solution, although some initial conditions consisted of a balanced profile with half of the electrode in a state on the upper branch of the slow manifold and the other half in a state on the lower branch of the slow manifold (e.g., the one that resulted in the lower pattern of Fig. 6). This observation underlines that here rules different from those valid for classical two-phase CPs govern the relative size of each phase.

Third, the local oscillators within *any individual spatial domain* are different, not only those belonging to obviously different cluster states. This can be seen from the phase portraits displayed in Fig. 7. The oscillations are taken from the positions marked by arrows in the upper plate of Fig. 6(a). The first two phase portraits belong to two in-phase cluster domains, the lowest one to an out-of-phase domain. The
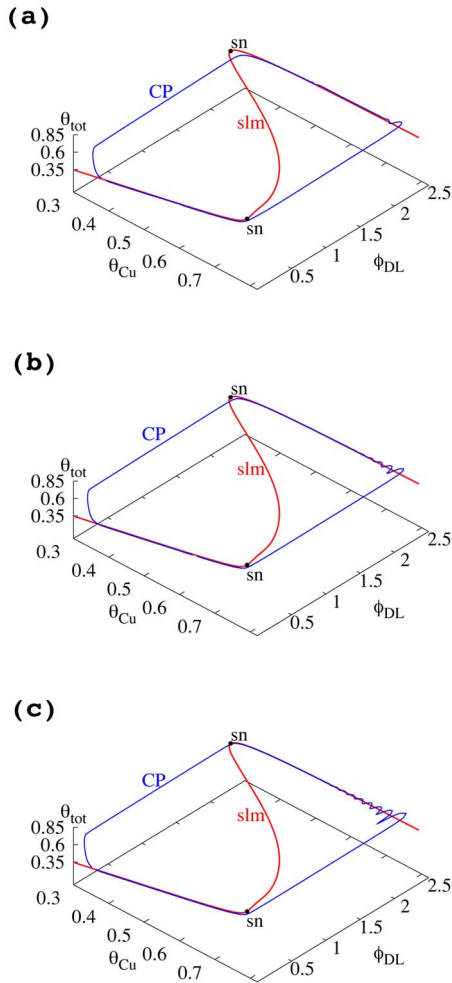
(a)

(b)

(c)

FIG. 7. (Color online) Trajectories in phase space of local oscillations (curves labeled CP) of the CP shown in Fig. 6(a) at the positions marked by the arrows. (a) $x=0.35\ \pi$, (b) plate $x=0.63\ \pi$, and (c) $x=1.37\ \pi$. The curves labeled slm are the slow manifold of the homogeneous system (for their calculation, see Sec. III).

(a)

(b)

(c)

FIG. 8. (Color online) Upper plate: Local time series of ϕ_{DL} and i_m [see Eq. (1) or Eq. (6)] of the CP shown in Fig. 6(a) at locations in antiphase domains: $x=1.37\ \pi$ (A and D labeled curves), $x=0.64\ \pi$ (B and C labeled curves). Middle plate: As upper plate but for two time series in in-phase domains: $x=1.37\ \pi$ (A and D labeled curves), $x=0.35\ \pi$ (B and C labeled curves). Lower plate: Local time series of ϕ_{DL} (E labeled curve) and θ_{Cu} (G labeled curve) at $x=0.35\ \pi$. The inset illustrates the effect a transition of the antiphase domain has on ϕ_{DL} and θ_{Cu} in the down state.

phase portraits exhibit different SAO fine structures and the transition from the upper state to the lower state on the slow manifold occurs at different locations. In Fig. 7(a), the SAOs are hardly discernible and the trajectory jumps from the upper to the lower branch of the slow manifold at a considerable distance from the sn. In Fig. 7(c), the SAOs are most pronounced and the transition to the lower branch occurs at the fold of the slow manifold. In Fig. 7(b), we have an intermediate situation. This trend correlates with the size of the individual domains: The smaller the domain, the more damped the SAOs and the farther away is the distance between jump state and sn bifurcation on the upper branch of the slow manifold. This correlation was found in all our calculations.

Further characteristics of the CPs can be extracted from local time series of ϕ_{DL} and i_m (Fig. 8). Figure 8(a) displays these quantities for two positions that oscillate out of phase, Fig. 8(b) for two in-phase oscillations in different domains. Figure 8(c), finally, displays time series of different variables at one position. Several observations can be made: First, an oscillator is much longer in a low-potential state than in a
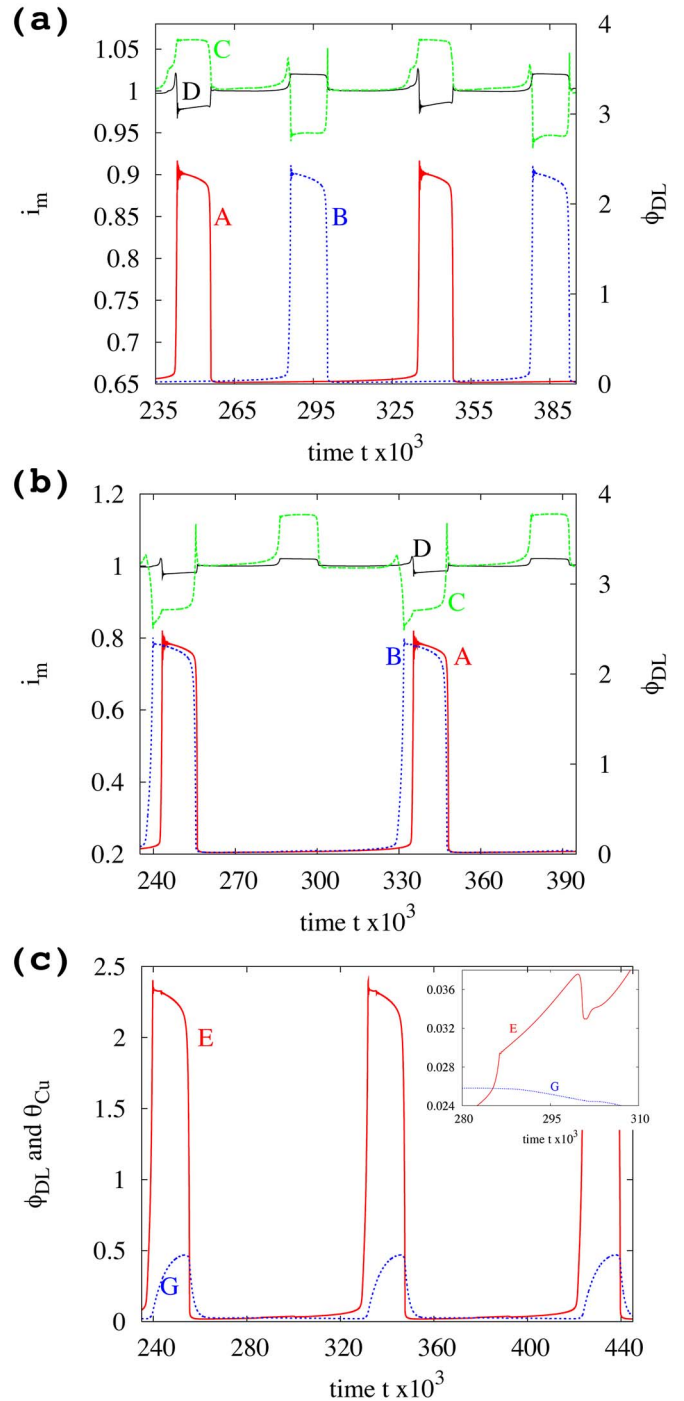
high-potential state, in contrast to the typical uniform MMOs in this parameter range, which display exactly the opposite behavior [cf. Fig. 2(a)]. As a consequence, over a considerable fraction of an oscillation period, both oscillators are in a low-potential state.

Second, the local time series of the migration current density displays not just two but three distinct levels. If we denote a state on the upper stable branch of the manifold as an "up-state" and one on the lower branch as a "down-state," three states can be distinguished: (a) Cluster one is in the up-state and cluster 2 in the down-state, (b) both clusters are in the down-state, and (c) cluster 2 is in the up-state and cluster 1 in the down-state. The local migration current reflects these three states: it is lowest when ϕ_{DL} at the same position is in an up-state, it takes on an intermediate value when both domains are in the down-state, and it jumps to a higher value when the out-of-phase domains jump to the up-state. Furthermore, when both clusters are in the down-state, the local current densities in both clusters are approximately equal and close to the galvanostatically preset current density, implying that in the down-down-state the entire electrode is nearly uniform. In Ref. 29, two different kinds of two-phase clusters were reported: The "classical" ones, termed type-I clusters, in which both states always oscillated approximately 180° out-of-phase and whose spatio-temporal structure could be captured by considering a single spatial "cluster mode," the system's dynamics switching between up-down and down-up configurations; and more unusual ones, denoted as clusters of type-II, in which the phase difference between the two clusters oscillated between approximately +90° and −90° and whose spatio-temporal behavior could only be reproduced with the superposition of a uniform and a cluster mode. The above compiled characteristics of our CPs suggest that they constitute clusters of type-II.

In Fig. 8(b), local time series of i_m and ϕ_{DL} are shown for two positions belonging to different "in-phase" regions. This representation reaffirms that the oscillators of different regions, even if they are nearly synchronized, are not identical. In addition, it can be seen that the transition to the up-state occurs at different points in time while they concomitantly return to the down state. Furthermore, they exhibit greatly different levels of i_m in the up-down states as well as in the down-up states. In general, we observed that the difference of i_m from the preset current density is larger the smaller the domain is. The magnification shown as an inset in Fig. 8(c) reveals that ϕ_{DL} in a down domain changes slightly upon a transition of the other state to an up-state, while θ_{Cu} and θ_{Cl} (not shown for clarity) remain essentially unaffected. Hence, the difference in migration current density when an antiphase domain is in the up-state is only caused by a slightly different value of ϕ_{DL}. This helps in our further discussion of the origin of the unusual CP features.

At this point, it is useful to summarize the properties of the CPs: (i) There is a multiplicity of patterns with different fractions of the electrode in the two anticorrelated states and different oscillation periods. (ii) None of the patterns exhibits phase balance. (iii) The limit cycles of every individual domain are different. (iv) The SAOs of a fast subsystem present in the lumped system are strongly suppressed in the local oscillations of a CP in the spatially extended system.

To get further insight in the origin of these properties, let us assume that to a first approximation, the thickness of the interfacial regions between "up" and "down" domains can by neglected. Normalizing space to 1, and denoting the sum of all domains that are in the up-state by y, $(1-y)$ is the length of all domains in the down state. If, for simplicity, we assume that the local migration current density of all domains in one state is equal, the galvanostatic control requires that

$$i_m^{up} y + i_m^{down}(1-y) = i_0 = y(i_0 - i^{up}) + (1-y)(i_0 + i^{down}),$$

where $i_m^{up\ (down)}$ are the migration current densities of the domains in the up- (down-) state and we have introduced the following definitions:

$$i^{up} \equiv i_0 - i_m^{up}; i^{down} \equiv i_m^{down} - i_0.$$

Phase balance would be achieved when $y = 0.5$ and thus

$$|i^{up}| = |i^{down}|,$$

i.e., the absolute value of the deviations of the migration densities from the preset current density had to be the same for both states. This constitutes a constraint that should hold only in exceptional cases, if at all. From these simple considerations, we can thus conclude that in general the galvanostatic control conditions prevent the system from taking on a phase-balanced state. In fact, in systems in which phase balance was observed, the global coupling was introduced as a feedback that did not impose a further constraint on the systems. These considerations make it likely that our result can be generalized and that phase balance will not be adjusted in globally coupled systems with constraints.

A further understanding of the properties of the CPs can be obtained when rewriting the migration current density in Eq. (1) in the following way:[18,20]

$$-\frac{\sigma}{\beta} \left.\frac{\partial\phi}{\partial z}\right|_{z=0} = i_m = i_0 + \frac{\sigma}{\beta}(\langle\phi_{DL}\rangle - \phi_{DL}) - \frac{\sigma}{\beta}\left.\left(\frac{\partial\phi}{\partial z} - \phi\right)\right|_{z=0}. \tag{6}$$

Here, galvanostatic control is assumed and i_m has been split into three contributions: (a) the current density that flows also in a uniform situation and is thus part of the local or homogeneous dynamics [cf. Eq. (5)]; (b) a contribution that constitutes a global coupling; it originates form the galvanostatic control, vanishes in a homogeneous situation, and is synchronizing; and (c) a term that accounts for spatial coupling through the electric field in the electrolyte, so-called migration coupling. In electrochemical systems, it represents the dominant spatial coupling and is nonlocal and synchronizing.

With Eq. (6), we can deduce that the fact that local trajectories in out-of phase domains correspond to different limit cycles is a consequence of the fact that phase balance is not fulfilled: The average double-layer potential depends on whether the smaller or the larger region is in the up- or down-state. Thus, the contribution of the global coupling term to the temporal evolution of ϕ_{DL} in one state is different from the contribution of this term to the other state half a period later. However, if the effective evolution equations are different, the resulting limit cycles cannot be expected to be the same. Note that in addition, the contribution of the migration coupling to the evolution equations of states in the two domains with antiphase behavior will be different.

Focusing again on the global coupling term, we can also provide a heuristic argument why the SAOs are strongly damped in our CPs. The SAOs of the up-state cause the average double-layer potential $\langle \phi_{DL} \rangle$ to oscillate with the same frequency. Thus all positions in the down-state experience a periodic forcing that will cause at least slightly changed values of i_m. To still fulfill the galvanostatic condition, this change has to be compensated by a change of equal magnitude of the sum of capacitive and faradaic current in the down domains. This, again, constitutes a constraint that is unlikely to be met for exactly the same reason as phase balance will not adjust. This heuristic argument seems to be likely to hold in general for relaxation oscillators with a fast oscillatory subsystem and a global constraint, but certainly calls for a more rigorous treatment.

From Eq. (6) it is apparent that two synchronized domains, though being on different limit cycles, experience the same contribution of the global coupling term when an antiphase domain undergoes a transition from the down-state to the up-state, as, e.g., at time 280 in Fig. 8, since their local values of ϕ_{DL} are essentially the same. The different response in i_m of the two domains is thus necessarily a consequence of the migration coupling. The latter is nonlocal and therefore affects the entire region of small adjacent domains while its impact on large domains is less significant. The different repercussion of migration coupling on the individual domains thus also causes the oscillators of synchronized states to adjust to different limit cycles in phase space. Moreover, the configuration of the individual domains matters, not only the fraction of the spatial domain that is in one state. These facts underline that even though the nature of the pattern is dominated by global coupling, in the case of nonlocal coupling, pattern selection is governed by intricate rules. This is apparently in contrast to globally coupled reaction-diffusion systems, where it is believed that the only effect of diffusion is to introduce a minimum domain size; otherwise, all configurations of domains are equally stable as long as the total fraction of the domains remains equal.

V. CONCLUSIONS

With a specific electrochemical model, we demonstrated that the properties of two-state CPs are more intricate than earlier studies on CPs in spatially extended systems revealed. These features result from a combination of the properties of the homogeneous oscillations in the model and the spatial coupling. The oscillations of the lumped system were relaxation-like, the system spending most of the time on the stable branches of an S-shaped slow manifold. One of the stable branches had an oscillatory inset, which led to MMOs in part of the parameter space, the dynamics being thus intrinsically three-dimensional. A synchronizing global coupling was imposed by a global constraint, and different regions in space were in addition coupled nonlocally with each other.

The global constraint was shown to prevent the two domains with antiphase behavior from taking up equal total regions in space. Thus, phase-balanced solutions, as they were found to be characteristic in systems with a global feedback, do not exist. It also causes the oscillations within two antiphase domains to occur on different limit cycles, and it suppresses the SAOs around one state of the slow manifold. The nonlocal coupling, in turn, forces the oscillations in different synchronized regions to occur on different limit cycles. This also implies that size and number of individual regions matter, not only the entire size a domain state occupies. In addition, a multiplicity of states is found, different patterns being characterized by different fractions of space that are occupied by each of the two domain states and by different frequencies.

The results prompt a number of questions. The most obvious one is how far the results can be generalized. In other words, it would be desirable to put the results on a more general basis using normal form type equations. Another question concerns the period of a cluster state if the underlying homogeneous oscillations are relaxation-like. It is clear that in this case the lumped oscillator will generically spend different fractions of the oscillation period on each of the stable branches of the slow manifold, implying that in a cluster state the local oscillations must somehow adjust their periods. Further questions concern the conditions a system has to fulfill such that it can support phase-balanced solutions, or what kind of qualitatively different patterns are possible in systems with a local dynamics that is intrinsically three-dimensional. This includes, besides the bursting oscillations considered here, MMOs arising through other mechanisms, such as canards or Shil'nikov homoclinic loops, or chaotic oscillations. This still incomplete listing shows that our knowledge on pattern formation in spatially extended systems with global coupling is still quite fragmentary. It is a challenge for future work to tackle the above questions and to fill this gap.

[1] J. L. Hudson and T. T. Tsotsis, Chem. Eng. Sci. **49**, 1493 (1994).
[2] K. Krischer, in *Modern Aspects of Electrochemistry*, edited by B. E. Conway, J. O'M. Bockris, and R. White (Kluwer Academic/Plenum, New York, 1999), Vol. 32, pp. 1–142.
[3] M. Schell and F. N. Albahadily, J. Chem. Phys. **90**, 822 (1989).
[4] F. N. Albahadily, J. Ringland, and M. Schell, J. Chem. Phys. **90**, 813 (1989).
[5] K. Krischer, M. Lübke, W. Wolf, M. Eiswirth, and G. Ertl, Ber. Bunsenges. Phys. Chem. **95**, 820 (1991).
[6] M. T. M. Koper and P. Gaspard, J. Chem. Phys. **96**, 7797 (1992).
[7] M. T. M. Koper, P. Gaspard, and J. H. Sluyters, J. Chem. Phys. **97**, 8250 (1992).
[8] M. T. M. Koper and P. Gaspard, J. Phys. Chem. **95**, 4945 (1991).
[9] K. Krischer, M. Lübke, M. Eiswirth, W. Wolf, J. L. Hudson, and G. Ertl, Physica D **62**, 123 (1993).
[10] I. Z. Kiss, Science **296**, 1676 (2002).
[11] I. Z. Kiss and J. L. Hudson, Chaos **13**, 999 (2003).
[12] N. Mazouz, G. Flätgen, and K. Krischer, Phys. Rev. E **55**, 2260 (1997).
[13] H. Varela, C. Beta, A. Bonnefont, and K. Krischer, Phys. Rev. Lett. **94**, 174104 (2005).
[14] F. Plenge, H. Varela, and K. Krischer, Phys. Rev. Lett. **94**, 198301 (2005).
[15] F. Plenge, H. Varela, and K. Krischer, Phys. Rev. E **72**, 066211 (2005).
[16] J. Christoph and M. Eiswirth, Chaos **12**, 215 (2002).

[17] J. Christoph, P. Strasser, M. Eiswirth, and G. Ertl, Science **284**, 291 (1999).
[18] N. Mazouz, G. Flätgen, K. Krischer, and I. G. Kevrekidis, J. Electrochem. Soc. **145**, 2404 (1998).
[19] P. Grauel, J. Christoph, G. Flätgen, and K. Krischer, J. Phys. Chem. B **102**, 10264 (1998).
[20] K. Krischer, H. Varela, A. Birzu, F. Plenge, and A. Bonnefont, Electrochim. Acta **49**, 103 (2003).
[21] K. Krischer, in *Advances in Electrochemical Science and Engineering*, edited by R. C. Alkire and D. M. Kolb (Wiley-VCH, Weinheim, 2003), Vol. 8, p. 89.
[22] F. Plenge, H. Varela, M. Lübke, and K. Krischer, Z. Phys. Chem. **217**, 365 (2003).
[23] A. C. Hindmarsh, SIGNUM Newsl. **15**, 10 (1980).lsode is available from the netlib library http://www.netlib.org/odepack/
[24] E. M. Izhikevich, Int. J. Bifurcation Chaos Appl. Sci. Eng. **10**, 1171 (2000).
[25] R. Straube, D. Flockerzi, S. C. Muller, and M. J. B. Hauser, Phys. Rev. E **72**, 066205 (2005).
[26] L. Yang, M. Dolnik, A. M. Zhabotinsky, and I. R. Epstein, Phys. Rev. E **62**, 6414 (2000).
[27] M. Pollmann, M. Bertram, and H. H. Rotermund, Chem. Phys. Lett. **346**, 123 (2001).
[28] M. Bertram and A. S. Mikhailov, Phys. Rev. E **63**, 066102 (2001).
[29] H. Varela, C. Beta, A. Bonnefont, and K. Krischer, Phys. Chem. Chem. Phys. **7**, 2429 (2005).